# Quad-Band Electrically Small Dual-Polarized ZOR Antenna with Improved Bandwidth using Single-Split Ring Resonators and Spiral Slots Enabled with Reflector for GPS/UMTS/WLAN/WiMAX Applications

Mohammad Ameen(1), and Raghvendra Kumar Chaudhary*(2)
(1),(2)Department of Electronics Engineering, Indian Institute of Technology (Indian School of Mines), Dhanbad, India
(1)mohammadmn61@gmail.com, and (2)raghvendra.chaudhary@gmail.com*

## Abstract

An electrically small quad-band metamaterial (MTM) antenna based on the short-ended configuration of zeroth order mode (ZOR) added with a reflector unit cell presented in this paper. The antenna is highly miniaturized due to the ZOR mode and the addition of the CPW backed ground plane. The intended antenna electrical size is $0.094\ \lambda_0 \times 0.112\ \lambda_0 \times 0.006\ \lambda_0$ at 1.54 GHz and a physical dimension of $18.5 \times 22 \times 1.27$ mm$^3$. A bandwidth of 3.89%, 10.11%, 13.48%, and 30.76% is acquired for the four bands centered at 1.54 GHz, 2.57 GHz, 3.48 GHz, and 5.33 GHz and a CP bandwidth of 8.32% is obtained in the fourth band. Moreover, the antenna exhibits a good level of compactness, good axial ratio, good radiation efficiency, and acceptable $S_{11}$ bandwidth. The intended antenna is the best candidature for use in 1.5 GHz GPS L2 band, 2.6 GHz UMTS, 5.2/5.8 WLAN, and 3.3/3.6 WiMAX applications.

## 1. Introduction

In the new world, due to the technology advancements and their emerging applications, the demand for wireless systems and their associated systems are increased. Current technologies are demanding on compact and multiple functionality devices or systems with minimum cost with less utilization of space. Metamaterials (MTMs) are the well-emerging candidature for the design and development of compact microwave antennas [1] due to their remarkable inherent properties which are not been observed in right-handed (RH) materials. MTM utilizes composite right/left-handed (CRLH) transmission line (TL) structures for obtaining zeroth order resonance (ZOR) mode for device miniaturization [1]–[2]. Some of the antennas implemented by MTM concepts utilizes ENG-TL [2], CRLH mushroom [3], Mushroom with curved branches [4], CRLH-TL with SRR loading [5], and patch and CRLH-TL EBG [6].

In this newly designed antenna, an asymmetric co-planar waveguide (ACPW) fed electrically small ($ka = 0.46<1$) quad-band and dual-polarized MTM based antenna is described. Further, some new bandwidth improvement techniques are also introduced using single-split ring resonator (S-SRR) and spiral slots. Finally, the antenna is combined with a reflector for achieving the higher gain.

## 2. Antenna Design Methodology

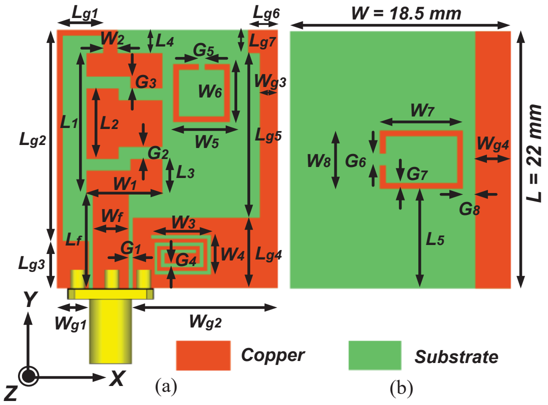

**Figure 1.** Simplified view of the designed quad-band dual-polarized MTM antenna. (a) upper view, and (b) back view.

The new configuration upper and back view of the intended MTM antenna with design dimensions is described in Figure 1. The antenna uses Rogers low loss RT-6006 substrate with $\varepsilon_r = 6.15$ and $tan\ \delta = 0.0027$ with a height of 1.27 mm. The design mainly consists of a feed line of length $L_f$ and width $W_f$ with ACPW feeding scheme is used for achieving wider bandwidth. The feed line is directly connected to a staircase shaped capacitor of width $G_2$ for realizing the series capacitor ($C_{L1}$). Then a rectangular patch ($L_1 \times W_1$) for realizing series inductance ($L_{R1}, L_{R2},$ and $L_{R1,}$) is introduced, then one more inverted staircase shaped series capacitor of gap $G_2 = 1$ mm is introduced. For shunt inductor ($L_L$), a small rectangular strip ($W_2 \times L_4$) is added and it is then directly connected with the ACPW ground plane. The gap separating the strip and the ACPW ground ($L_{G1}$) creates a shunt capacitor ($C_R$). For multiple bands and extending the bandwidths, two additional S-SRR and a spiral slot are added in the design. Further, a rectangular strip ($L \times W_{G4}$) added to the backside of ACPW ground plane for obtaining additional antenna compactness [7] and the generation of one more resonance. Figure 2 elaborates the design stages of quad-band antenna and Figure 3 shows the $S_{11}$ responses. The total antenna size is $18.5 \times 22 \times 1.27$ mm$^3$ with an electrical size of $0.094\ \lambda_0 \times 0.112\ \lambda_0 \times 0.006\ \lambda_0$ at 1.54 GHz. The antenna simulations and parametric studies are done by CST Microwave studio software.

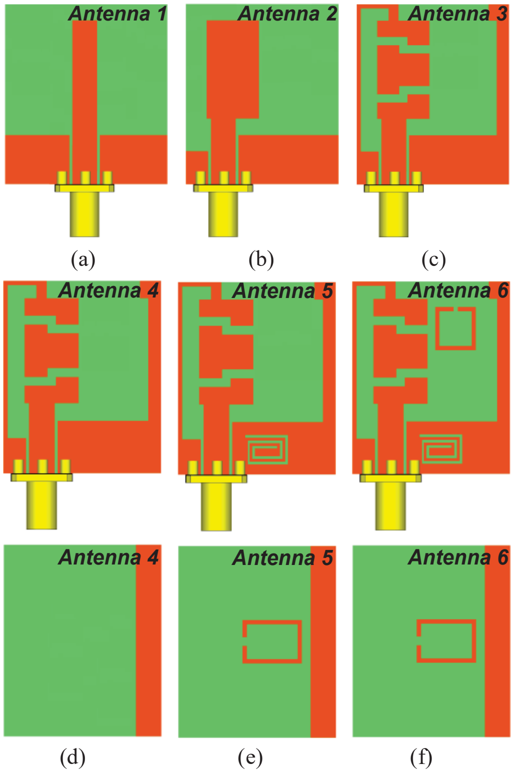

(a) (b) (c)

(d) (e) (f)

**Figure 2.** Antenna design stages, (a) Symmetric CPW feed, (b) ACPW feed with patch, (c) ACPW feed with CRLH-TL, (d) CRLH-TL with the backed ground plane, (e) S-SRR and spiral slots for bandwidth extension, and (f) S-SRR on top of the patch for CP generation.

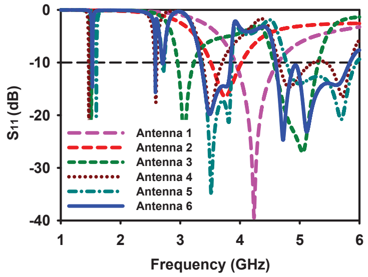

**Figure 3.** Return loss ($S_{11}$) characteristics for the quad-band antenna for design stages as exhibited in Figure 2.

The optimized antenna dimensions are $L = 22$, $L_f = 8$, $L_1 = 12$, $L_2 = 6$, $L_3 = 3$, $L_4 = 2$, $L_5 = 8.5$, $L_{g1} = 3.9$, $L_{g2} = 18$, $L_{g3} = 4$, $L_{g4} = 6$, $L_{g5} = 14$, $L_{g6} = 2.5$, $L_{g7} = 2$, $W = 18.5$, $W_f = 3$ , $W_1 = 6.35$, $W_2 = 1.2$, $W_3 = 5$, $W_4 = 3.35$, $W_5 = 4.75$, $W_6 = 4.95$, $W_7 = 7$, $W_8 = 5$, $W_{g1} = 2.6$, $W_{g2} = 12.1$, $W_{g3} = 1.5$, $W_{g4} = 3$, $G_1 = 0.4$, $G_2 = G_3 = G_6 = G_8$, $G_4 = 0.3$, $G_5 = 0.5$, and $G_7 = 0.5$ (All dimensions are in mm).

## 2.1 Equivalent Circuit Model of the Antenna

The equivalent circuit representation of the intended MTM single antenna is described in Figure 4. It consists of various lumped elements to represent the proposed design (Antenna 6). The antenna presented here is based on short-ended termination of CRLH-TL [1]. Series parameters are responsible for the ZOR frequency represented by a dotted red line in Figure 4. The ZOR frequency is given by (1),

$$f_{ZOR} = \frac{1}{2\pi\sqrt{(L_{R1} + L_{R2} + L_{R3})\left(\frac{C_{L1}\,C_{L2}}{C_{L1} + C_{L2}}\right)}} \qquad (1)$$

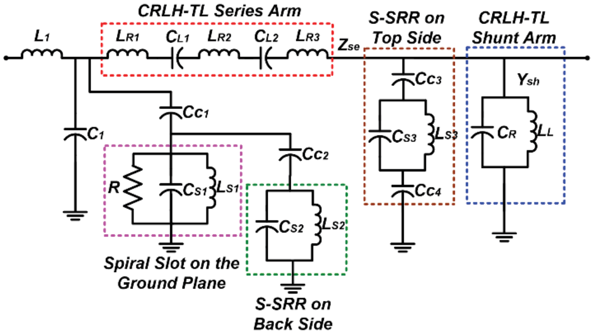

**Figure 4.** Equivalent circuit representation for the intended single antenna (Antenna 6) showing lumped elements.

## 2.2 MTM Antenna Design

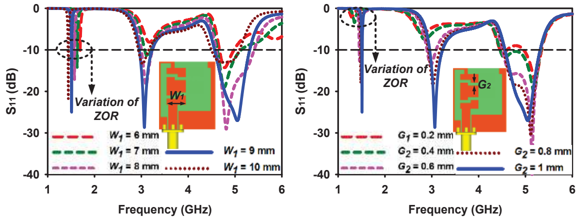

(a) (b)

**Figure 5.** Simulated $S_{11}$ characteristics of the MTM antenna. (a) Variation of $W_1$, and (b) Variation of $G_2$.

Consider the Antenna 3 in Figure 2(c) to verify the MTM behavior of the single antenna, Figure 5(a) represents the variation of series inductance on increasing $W_1$ and it is to be found that increasing $W_1$ shifts the ZOR to lower frequency due to the increase in effective inductance. Similarly Figure 5(b) shows the variation of series capacitance by varying $G_2$ and it is found that increasing $G_2$ ZOR shifts to higher frequency due to decreasing capacitance and an optimum value of $G_2 = 1$ mm is chosen. It is to be noted that there is no variation in resonances for the change in the shunt parameters. Hence it is understood that the antenna exhibits MTM property.

## 2.3 Bandwidth Extension of MTM Antenna

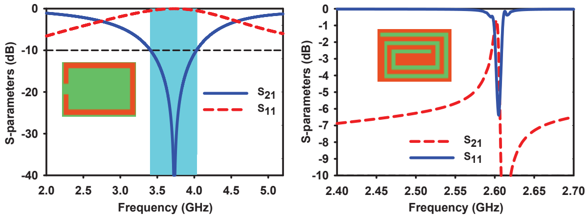

(a) (b)

**Figure 6.** Unit cell responses. (a) The response of S-SRR at 3.6 GHz, and (b) Response of spiral slots at 2.6 GHz.

Consider the Antenna 5 in Figure 2(e), an additional spiral-shaped slot in the ACPW ground plane and S-SRR introduced in the back side enhances the bandwidth of the second and third resonance frequencies by merging the additional resonances due to S-SRR and spirals. The corresponding response of S-SRR at 3.6 GHz is described in Figure 6(a) and, the response of the spiral slots are described in Figure 6(b) indicating that additional S-SRR and spiral slots can achieve extended bandwidth.

## 2.4 Reflector Backed MTM Antenna for High Gain and Axial Ratio Improvement

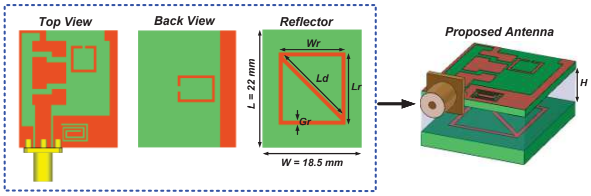

**Figure 7.** Schematic overview of the proposed reflector backed dual polarized MTM antenna.

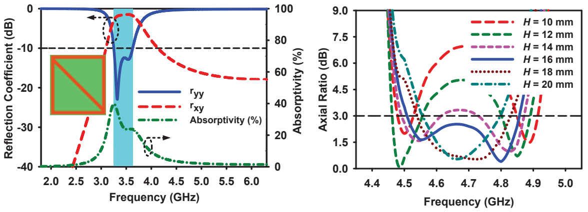

(a) (b)

**Figure 8.** Unit cell characteristics (a) reflector transmission and reflection plot with absorptivity, and (b) Variation of the axial ratio by varying *H*.

In order to boost the radiation characteristics such as ARBW and gain of the antenna a reflector based LP to CP converter is placed below the radiator antenna (Antenna 6). A foam layer ($\varepsilon_r = 1$) is used for mechanical support with $H = 16$ mm. Below the foam layer FR-4 substrate with $\varepsilon_r = 4.4$ and $\tan\delta = 0.02$, with a height of 3.2 mm is used as a substrate for the reflector. The schematic overview is depicted in Figure 7. The dimensions are $L_d = 15.44$ mm, $L_r = 13.45$ mm, $G_r = 0.75$ mm and $W_r = 12.45$ mm. Figure 8(a) exhibits the unit cell transmission, reflection, and absorption plots and it is clearly understood that the unit cell, the absorption is very less at 3.6 GHz and hence it will act as a reflector at 3.6 GHz for use in WiMAX application. Figure 8(b) shows the variation of the axial ratio by adjusting the spacing between the radiator MTM antenna and reflector and it is found to be more ARBW is obtained at $H = 16$ mm.

## 3. Results and Discussions

The measured reflection coefficient ($S_{11}$) and simulated axial ratio plot of the intended MTM antenna are described in Figure 10 with bandwidths of 60 MHz (1.51–1.57 GHz), 260 MHz (2.44–2.70 GHz), 470 MHz (3.25–3.72 GHz) and 1640 MHz (4.51–6.15 GHz) for the four bands respectively with percentage bandwidths of 3.89%, 10.11%, 13.48%, and 30.76% as displayed in the Figure 10(a). For the fourth band an ARBW of 390 MHz (4.49–4.88 GHz) with a percentage ARBW of 8.32% depicted in Fig. 10(a).

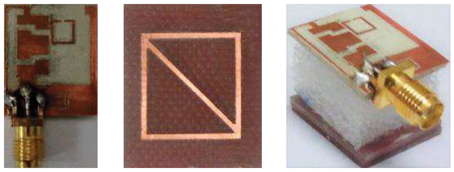

(a) (b) (c)

**Figure 9.** Fabricated antenna prototype. (a) MTM antenna, (b) LP to CP converter, and (c) Final antenna prototype.

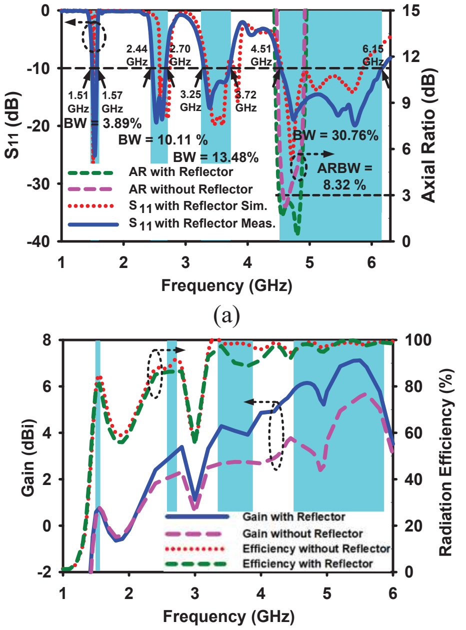

(a)

(b)

**Figure 10.** Simulated far-field results for the intended antenna (a) $S_{11}$ and AR, and (b) gain and radiation pattern.

The gain and radiation efficiency also simulated and plotted in Figure 10(b). A gain of 0.75 dBi, 2.89 dBi, 4.28 dBi, and 7.12 dBi is obtained at the four bands. Here a significant amount of gain is improved by 0.92 dBi in the second band, 1.6 dBi in the third band, and 1.57 dBi for the fourth band. The simulated radiation efficiency is 81.15%, 86.29%, 90.15%, and 96.01% are obtained for the four frequencies respectively. The radiation pattern is also plotted as depicted in Figure 11. It shows bidirectional pattern in the *xz*-plane and omnidirectional pattern in *yz*-plane at 1.55 GHz and 2.6 GHz as shown in Figure 11(a) and 11(b). Because of reflector in the design, directional pattern observed in the *xz*-plane and *yz*-plane for 3.6 GHz, 5.2 GHz, and 5.5 GHz as shown in the Figure 11(c), Figure 11(e) and Figure 11(f) respectively. It is to be noted that at 4.7 GHz CP is achieved and it shows left-handed circular polarization radiation as shown in Figure 10(d). Table. 1 depicts the comparison between the existing dual polarized MTM antennas with the proposed antenna results.

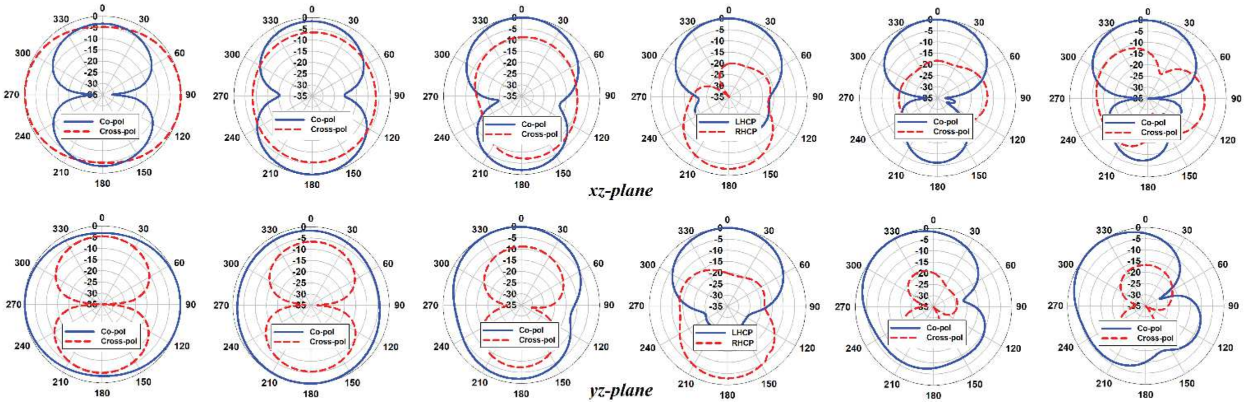

(a) (b) (c) (d) (e) (f)

**Figure 11.** Simulated radiation pattern of the quad-band MTM antenna (a) 1.55 GHz, (b) 2.6 GHz, (c) 3.6 GHz, (d) 4.7 GHz, (e) 5.2 GHz, and (f) 5.5 GHz.

**Table. 1** Comparitive study between the designed quad-band antenna with existing MTM antennas.

| Ref. No. | Freq. (GHz) | Antenna Dim. ($mm^3$) | *Ka* | BW (%) | Axial Ratio (%) | Gain (dBi) |
|---|---|---|---|---|---|---|
| [3] | 2.89 | 60 × 60 × 3.175 | 2.58 | 2.94 | 0.41 | 6.26 |
| | 3.82 | | | 0.62 | 0.90 | 6.97 |
| [4] | 1.85 | 70 × 70 × 3.175 | 1.91 | 0.49 | NA | -0.24 |
| | 2.86 | | | 1.33 | NA | -0.51 |
| [5] | 1.95 | 24.8 × 22 × 1.6 | 0.68 | 1.28 | - | -6.9 |
| | 2.61 | | | 5.3 | 0.7 | -1.1 |
| [6] | 1.33 | 70 × 70 × 2.5 | 1.38 | 1.88 | - | 2.1 |
| | 1.8 | | | 3.24 | - | 0.6 |
| | 2.41 | | | 10.03 | 1 | 5.7 |
| **MTM CP Ant.** | **1.55** | **18.5 × 22 × 1.27** | **0.46** | **0.65** | **-** | **0.77** |
| | **2.66** | | | **4.7** | **-** | **2.06** |
| | **3.6** | | | **14.03** | **-** | **2.68** |
| | **5.2** | | | **24.04** | **1** | **5.55** |
| **MTM CP + Reflector** | **1.54** | **18.5 × 22 × 16** | **0.72** | **3.89** | **-** | **0.75** |
| | **2.57** | | | **10.11** | **-** | **2.89** |
| | **3.48** | | | **13.48** | **-** | **4.28** |
| | **5.33** | | | **30.76** | **8.32** | **7.12** |

## 4. Conclusion

A miniaturized and low profile quad-band, dual-polarized MTM antenna is designed and explained. The antenna obtain miniaturized size of $0.094\lambda_0 \times 0.112\lambda_0 \times 0.006\lambda_0$ at 1.54 with $ka = 0.46 < 1$due to ZOR property. The antenna size is compared with a conventional patch antenna and it is observed to be 80.84% size reduction in the radiating element is achieved. Moderate gain, wider bandwidth, and acceptable radiation pattern with miniaturized size shows that the designed antenna is suitable for work in the GPS L2 band (1.51–1.59 GHz), UMTS (2.5–2.69 GHz), WiMAX (5.15–5.725 GHz), (3.3–3.8 GHz), and WLAN (5.15–5.825 GHz) application systems.

## 5. Acknowledgements

This research work is supported by Science and Engineering Research Board (SERB), DST, Government of India under grant number EEQ/2016/000023.

## 6. References

1. A. Lai, K. M. K. H. Leong, and T. Itoh, "Infinite Wavelength Resonant Antennas with Monopolar Radiation Pattern Based on Periodic Structures," *IEEE Trans. Antennas Propag.*, **55**, 13, March 2007, pp. 868–876, doi: 10.1109/TAP.2007.891845.

2. M. Ameen, and R. K. Chaudhary, "Metamaterial Based Circularly Polarized Antenna Employing ENG-TL with Enhanced Bandwidth for WLAN Applications," *Electronics Lett.*, **54,** October 2018, pp. 1152–1154, doi: 10.1049/el.2018.5701.

3. S. T. Ko, B. C. Park, and J. H. Lee, "Dual Band Circularly Polarized Patch Antenna with First Positive and Negative Modes," *IEEE Antennas and Wireless Propag. Lett.*,**12**, September 2013, pp. 1165–1168, 10.1109/LAWP.2013.2281320.

4. B. C. Park, and J. H. Lee, "Dual Band Omnidirectional Circularly Polarized Antenna using Zeroth- and First-Order Modes," *IEEE Antennas and Wireless Propag. Lett.*, **11**, July 2012, pp. 407–410, doi: 10.1109/LAWP.2012.2193550.

5. C. Zhou, G. Wang, Y. Wang, B. Zong, and J. Ma, "CPW-Fed Dual-Band Linearly and Circularly Polarized Antenna Employing Novel Composite Right/left-handed Transmission line," *IEEE Antennas and Wireless Propag. Lett*., **12**, September 2013, pp. 1073–1076, doi: 10.1109/LAWP.2013.2279689.

6. W. Cao, B. Zhang, A. Liu, T. Yu, D. Guo, and X. Pan, "Multi-Frequency and Dual Mode patch antenna based on Electromagnetic Band-Gap (EBG) Structure," *IEEE Trans. Antennas Propag.*, **60**, 12, December 2012,pp. 6007–6012, doi:10.1109/TAP.2012.2211554

7. S. K. Sharma, A. Gupta, and R. K. Chaudhary, "Epsilon Negative CPW-fed Zeroth-Order Resonating Antenna with Backed Ground for Extended Bandwidth and Miniaturization," *IEEE Trans. Antennas Propag.*, **63**, 11, November 2015, pp. 5197–5202, doi: 10.1109/TAP.2015.2477521.